Sustainable Food Technology

ROYAL SOCIETY OF CHEMISTRY

PAPER

View Article Online
View Journal | View Issue

Cite this: *Sustainable Food Technol.*, 2026, 4, 868

Optimization of supercritical fluid extraction of valuable compounds from *Lagerstroemia speciosa* leaves for *in vitro* antidiabetic and antioxidant activity

Kiran Khandare[ab] and Saswata Goswami *[a]

This study reports, for the first time, the optimization of supercritical CO_2 extraction (SFE) of phenolic compounds from *Lagerstroemia speciosa* (*LS*) leaves using Response Surface Methodology (RSM), targeting both antioxidant and antidiabetic potential. Unlike conventional solvent-based extractions, SFE offers a green and tunable approach to recover thermolabile bioactive compounds. The extraction was optimized by varying pressure (20–40 MPa), temperature (70–110 °C), and time (30–70 min). The optimal conditions, 29.59 MPa, 89.50 °C, and 53.85 min, yielded 99.31 ± 2.57 mg GAE per g dry biomass of total phenolic content (TPC). Ultra Performance Liquid Chromatography-Photodiode Array detector (UPLC-PDA) analysis confirmed the presence of key phenolics such as *p*-hydroxybenzoic acid, vanillic acid, *p*-coumaric acid, chlorogenic acid, and vanillin. The extract exhibited strong enzyme inhibitory activity with IC_{50} values of 30.09 ± 2.58 μg mL^{-1} and 59.45 ± 3.40 μg mL^{-1} against α-amylase and α-glucosidase, respectively, demonstrating its dual antioxidant and antidiabetic potential. These findings highlight *LS* leaves as a promising and underexplored source of bioactive compounds for the development of functional foods, nutraceuticals, and pharmaceutical applications.

Received 17th July 2025
Accepted 4th November 2025

DOI: 10.1039/d5fb00395d

rsc.li/susfoodtech

Sustainability spotlight

This study exemplifies a sustainable and green chemistry approach by utilizing supercritical carbon dioxide (SC-CO_2), a non-toxic, recyclable, and environmentally benign solvent, for the optimized extraction of phenolic compounds from *Lagerstroemia speciosa* leaves. Unlike conventional solvent-based methods that rely on hazardous organic solvents, our method minimizes environmental footprint while maximizing bioactive compound yield. The efficient extraction under moderate temperature and pressure conditions ensures the preservation of thermolabile compounds, supporting the clean-label movement and advancing the development of eco-friendly, plant-based functional ingredients for the pharmaceutical and nutraceutical industries.

1 Introduction

Phytochemicals benefit human health and are abundantly found in medicinal and aromatic plants. *Lagerstroemia speciosa* (Banaba) is a widely distributed tropical plant native to Asia and common in several Indian states, including Punjab, Haryana, and Himachal Pradesh. In the Philippines, Taiwan, and Japan, its leaves have long been used as a traditional remedy for diabetes. Owing to its ethnomedicinal significance and availability, *LS* represents a promising natural source for developing plant-based antidiabetic formulations. Typically, they are extracted with methanol : water mixtures, resulting in high gravimetric yields but somewhat non-selective and complicated extracts.[1,2]

In present scientific practices, volatile solvents carry out extractions, which usually require several hours or even more days. Besides, the extraction requires enormous amounts of such solvents, including methanol, acetone or other hazardous chemicals, which are not only toxic but also reduce the extraction efficiency by degrading thermolabile compounds.[3–5] SFE has been found to have broad applications in food, pharmaceutical, and chemical industries to extract bioactive compounds due to the non-toxic nature of CO_2. Applying CO_2 makes it possible to employ *LS* resources rationally by using a green solvent. Scientists, food producers, and consumers are particularly interested in phenolic compounds because of their impact on food quality and potential protective and preventative roles in the pathophysiology of various chronic diseases. Phenolic acids such as vanillin and *p*-coumaric acid are among the most significant bioactive compounds due to their strong antioxidant potential and diverse physiological roles. Vanillin exhibits antimicrobial, anti-inflammatory, and anticancer properties, while *p*-coumaric acid serves as a valuable fragrance

[a]*Division of Chemical Engineering, Center of Innovative and Applied Bioprocessing, Knowledge City, Sector-81, Mohali, Punjab, India-140306. E-mail: sasawatagoswami2015@gmail.com*
[b]*Department of Biochemistry, University Institute of Engineering and Technology, Panjab University, Chandigarh, India-160014*

and pharmaceutical precursor owing to its phenolic structure. In recent years, the demand for vanillin and *p*-coumaric acid has increased significantly, driven by consumers' preference for natural and organic food products.[6] For instance, the global natural vanillin market is projected to reach USD 706 million by 2027, with an annual growth rate of 8.4%.[7,8] Greener extraction methods have been developed for recovering vanillin and *p*-coumaric acid from natural sources. However, lignin-derived vanillin is difficult to purify compared to plant-based vanillin[9] and *p*-coumaric acid extracted from sugarcane bagasse shows low bioavailability due to fiber binding, making its pure form more effective.[10] Though our research did not focus on optimising the extraction of vanillin and *p*-coumaric acid, it is an effort to obtain high-quality vanillin and *p*-coumaric acid through their purification. Although numerous studies on vanillin and *p*-coumaric acid and their biological activities are known, no report has mentioned the presence of vanillin and *p*-coumaric acid in *LS*.

α-Amylase and α-glucosidase are key carbohydrate-hydrolyzing enzymes responsible for generating glucose from complex polysaccharides.[11] Their excessive activity contributes to postprandial hyperglycemia, which is associated with complications such as type 2 diabetes mellitus, obesity, cardiovascular disorders, nephropathy, neuropathy, and retinopathy.[12,13] Inhibiting these enzymes can therefore help regulate blood glucose levels. In this context, *LS* extracts were investigated for their potential antidiabetic activity, and their efficacy was compared with HP-20 purified vanillin and *p*-coumaric acid, known for their *in vitro* enzyme inhibition properties.

Conventional solvent extraction of *LS* often results in poor selectivity, longer processing time, and degradation of bioactives, while green alternatives such as SFE remain underutilized for this species. Therefore, there is a clear need to establish an environmentally sustainable and efficient process for high-quality extraction of phenolic compounds from *LS*. Thus, the objectives of this study were to (i) evaluate the most effective parameter to extract phenolic compounds from *LS*, (ii) screen significant extraction variables in SFE using a central composite design, (iii) identify and quantify the phenolic compounds using UPLC-PDA, (iv) purify the phenolic fractions using Diaion HP-20 column chromatography, and (v) evaluate *in vitro* antidiabetic and antioxidant activity of SFE extract, vanillin and *p*-coumaric acid.

2 Materials and methods

2.1. Reagents and solvents

Analytical-grade chemicals were used throughout the process. α-Amylase from porcine pancreas, α-glucosidase from *Saccharomyces cerevisiae*, 4-nitrophenyl-β-D-glucopyranoside (PNPG), starch, sodium phosphate monobasic (NaH_2PO_4), sodium phosphate dibasic (Na_2HPO_4), Folin–Ciocalteu reagent, aluminium chloride ($AlCl_3$), DPPH (2,2-diphenyl-1-picrylhydrazyl), and sodium carbonate were obtained from Sigma-Aldrich. 99.9% pure carbon dioxide (CO_2) was purchased from Sigma Gases, Mumbai, Maharashtra.

2.2. Plant material

Leaves of *LS* were collected from the Center of Innovative and Applied Bioprocessing (CIAB) campus, Mohali. The GPS coordinates of the collection site are 30.6497° N; 76.7396° E. Leaves were washed with running tap water to remove external dust and dried using a fluidized bed dryer at pilot scale (50 L capacity) at 45 °C until they retained 8–9% water content. The moisture was analyzed using an aczet MB 50, 220–230 V capacity moisture analyzer. The dried powder was passed through a mass collider followed by sieving through a 500 μm sieve to keep a consistent particle size in each experiment.

2.3. Biomass surface characterization pre- and post-extraction

Field Emission Scanning Electron Microscopy (FE-SEM, JEOL JCM 6000 Nikon Corporation, Japan) was carried out to compare the surface morphology of dried powder when extracted with high-pressure supercritical CO_2 (SC-CO_2) and before its exposure. The sample was spread on double adhesive tape fixed on a scanning electron microscope (SEM) aluminium stub, followed by gold sputter coating.

2.4. Supercritical CO_2 extraction of TPC

The extraction experiments were carried out using an SFE-Helix system from Allentown, USA, as schematically depicted in Fig. 1. In this extraction method, a twin-piston pump injects liquid CO_2 into the system after being supplied with a syphon tube from a CO_2 cylinder. The pump is capable of working at pressures of up to 69 MPa. A vessel for SFE could be fitted into this system. The fluid was brought to its supercritical condition through a preheater and an enclosing heating jacket. The flow rate was managed using a sturdy variable restrictor valve. The restrictor was warmed electrically to avoid sample clogging.

Before each run, the CO_2 line was preheated for 15 min to ensure temperature equilibration, and the system was pressurized to the desired extraction pressure using high-purity CO_2 (99.9%, Sigma Gases, Mumbai, India). Once stable flow and pressure were achieved, about 10 g of dried leaf sample was weighed and loaded into the 50 mL extraction vessel. About 1.5 g of glass wool was packed at both ends of the extraction basket, and the leaf sample was sandwiched to prevent the transfer of solid samples to the tubing and the system from clogging. All the extractions were carried out according to the parameters mentioned in Table 1. SFE started when the desired extraction pressure and temperature were reached, and the extract was collected in an amber glass bottle. The CO_2 flow rate was maintained at 2.0 ± 0.1 mL min^{-1}, and stability was verified with fluctuations not exceeding ±2% during each run. The outlet micro-metering valve (restricted valve) was set at 20 °C higher than the extraction temperature in every extraction. At the end of the experiments, the extracted solution was kept at room temperature to evaporate residual CO_2. The extract was stored at 4 °C until further analysis. Each experiment was carried out at least three times under identical parameters to ensure the results could be reproduced.

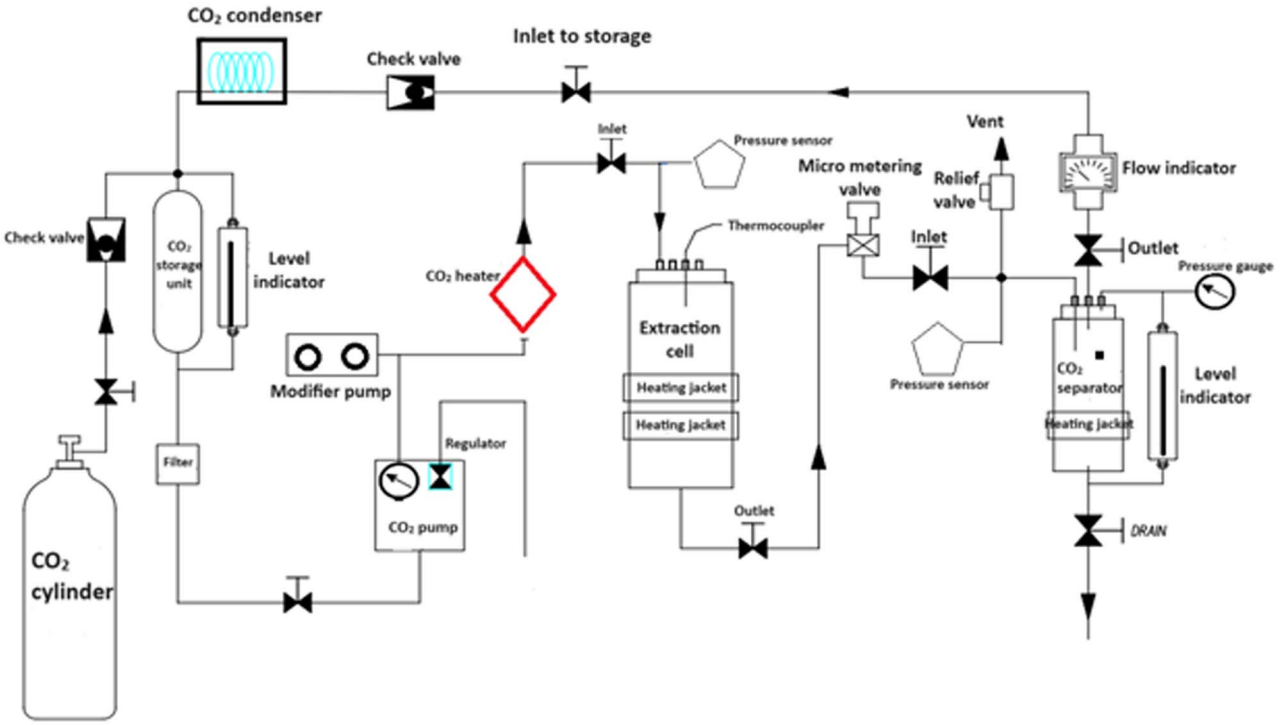

Fig. 1 The process flow of supercritical CO_2 extraction for total phenolic content (TPC).

Table 1 Coded and uncoded values of the parameters used in the experimental design

	Symbol		Coded levels		
Independent parameters	Coded	Uncoded	−1	0	1
Pressure (MPa)	X_1	P	20	30	40
Temperature (°C)	X_2	T	70	90	110
Extraction time (min)	X_3	ET	30	50	70

2.5. Determination of TPC using Folin–Ciocalteu colorimetric assay

The TPC of the extract was determined using the modified Folin–Ciocalteu method.[14] The 0.5 mL extract was mixed with Folin–Ciocalteau's reagent (Sigma Aldrich) (0.25 mL) and 1.25 mL of 20% sodium carbonate solution. The mixture was incubated for 40 min at room temperature. The optical density of the blue-coloured samples was measured at 725 nm using a UV2700 UV-visible spectrophotometer (Shimadzu, Kyoto, Japan). The TPC was expressed as mg of gallic acid equivalents per g dry weight of the biomass (mg GAE per g DWB) using gallic acid as a calibration standard. A calibration curve was constructed using concentrations ranging from 50 to 500 μg mL^{-1}. The curve showed a strong linear relationship between absorbance and concentration, obtained with the equation $y = 0.0009x + 0.0881$, with a correlation coefficient of $R^2 = 0.9945$. All measurements were carried out in triplicate, and the results are presented as mean ± standard deviation.

2.6. Determination of phenolic compounds using UPLC-PDA

Analysis of SFE-*LS* phenolic compounds was performed using an ultra-high performance liquid chromatography system developed on a UPLC-PDA system (Waters, Acquity H-Class, Milford, MA, USA) consisting of a quaternary solvent pump, an autosampler, a column port, and a PDA detector. The order of appearance on the chromatogram: benzoic acid, *p*-hydroxybenzoic acid, chlorogenic acid, vanillic acid, vanillin, syringic acid and *p*-coumaric acid were separated in a Zorbax Eclipse Plus C_{18} column (5 μm particle size, 250 mm length, and 4.6 mm internal diameter). Chromatograms were recorded in the 210–400 nm range, and peaks were integrated at 280 and 330 nm. The mobile phase consisted of 0.2% formic acid solution and 22% methanol. The samples were eluted using isocratic flow. Before injecting a new sample, the samples were run for 30 minutes to return to their initial conditions. The flow rate was 1 mL min^{-1}, and the injection volume was 10 μL. Each compound was identified based on its retention time by comparison with corresponding analytical standards under identical chromatographic conditions, showing retention times of *p*-hydroxybenzoic acid (9.91 min), chlorogenic acid (11.90 min), vanillic acid (13.33 min), vanillin (16.88 min), and *t*-coumaric acid (25.81 min), with minor variations across replicate injections (RSD < 2%), indicating consistent chromatographic performance. All results were expressed in mg per g DWB, representing the mean and standard deviation of three determinations. The analytical method was validated for linearity, precision, and accuracy following standard ICH guidelines.

Recovery experiments were performed by spiking known concentrations of standards into the matrix, yielding recoveries within 95–103%, indicating good accuracy and minimal matrix interference. Overall, the method demonstrated high reproducibility and suitability for the quantitative determination of phenolic compounds in the extract.

2.7. Pre-treatment of DIAION HP-20 resin

The pre-treatment of resin is crucial to get rid of trapped monomers and porogenic substances inside the pores during the synthesis process. The resin underwent a 24-hour methanol soak as a pre-treatment, and methanol was removed after the 24-hour treatment. The resin was cleaned twice with distilled water and submerged in 1 M NaOH for five hours. Then, again, the resin was washed twice with distilled water. The washed resin was soaked in 1 M HCl for five hours. Finally, the resin was washed with distilled water thoroughly and dried at 45 °C.

2.8. Purification of phenolic compounds using DIAION HP-20 column chromatography

The macroporous resin with weak polarity and a polystyrene structure having less than 0.25 μm particle size was used to purify the phenolic compounds. The SFE-*LS* extract was dissolved in 100 mL of distilled water for a final 5 mg mL^{-1} concentration of phenolic compounds. The 50 g of pre-treated resin was weighed and incubated with diluted SFE-*LS* extract for 24 h at room temperature. The resin was then set into a 500 mL glass column (1.5 × 9 cm). The unadsorbed material was carefully washed using distilled water. The dynamic desorption experiment was conducted. The resin was desorbed with 100 mL of 30% v/v, 50% v/v, 70% v/v and 90% v/v methanol concentration with the elution flow rate of 0.5 mL per minute, respectively. The fractions were concentrated using a rotary evaporator (Büchi Rotavapor R-300, Büchi Labortechnik AG, Flawil, Switzerland) under conditions of 45 °C water bath temperature, vacuum pressure of 100 mbar, and chiller temperature of 2 °C, and subsequently lyophilized using a freeze-dryer (Labconco FreeZone 2.5, Labconco Corporation, Kansas City, MO, USA) until a dry powder was obtained.

2.9. Structural elucidation of purified compounds

Nuclear magnetic resonance (NMR) spectroscopy of the purified compounds was carried out using ^{1}H NMR in deuterated solvent (DMSO-d_6) at room temperature on a Bruker Avance 500 spectrometer operating at 500 MHz. The spectra were acquired using a standard one-pulse sequence (zg30) with a relaxation delay of 1.0 s, a spectral width of 10 ppm, and 32 scans to ensure an adequate signal-to-noise ratio. The temperature was maintained at 298 K during all measurements.

2.10. Evaluation of antioxidant activity using the DPPH free radical-scavenging method

1 mL of 1 mM DPPH solution and 1 mL varied dilutions of test samples (250 μg mL^{-1} 1000 μg mL^{-1}) were mixed. The reaction was left in the dark for 30 min. The absorbance was later measured at 517 nm using a UV-visible spectrophotometer (Shimadzu, Kyoto, Japan).[15] Ascorbic acid was used as a reference standard. The radical-scavenging capacity of DPPH was determined as a radical inhibition concentration of 50% (IC_{50}).

For the DPPH assay, IC_{50} values (the concentration of extract required to scavenge 50% of DPPH radicals) were determined using *GraphPad Prism* (version 9.0, GraphPad Software, USA) as described in Section 2.12. The absorbance values at 517 nm were used to compute the percent radical-scavenging activity using the formula:

$$\text{DPPH free radical scavenging (\%)} = \frac{(\text{absorbance of control} - \text{absorbance of sample})}{\text{absorbance of control}} \times 100$$

The percent scavenging values were plotted against the logarithm of sample concentrations (μg mL^{-1}), and non-linear regression was applied using the four-parameter logistic (4PL) model (variable slope). The IC_{50} values and their 95% confidence intervals were extracted directly from the fitted dose–response curves. All experiments were conducted in triplicate, and the results were expressed as mean ± SD.

2.11. α-Amylase inhibitory activity

α-Amylase inhibitory activity was studied using the protocol described in ref. 16. 50 μL of the sample (250–1000 μg mL^{-1}) along with 50 μL of ≥2.5 U mL^{-1} α-amylase solution was taken in a centrifuge tube and incubated for 10 min at 25 °C. After incubation, 0.5% starch solution (50 μL) was added into the tube and incubated for 3 min at 25 °C. The mixture was boiled for 10 min after adding 100 μL of 3,5-dinitrosalicylic acid (DNS) colour reagent solution. Then, 100 μL of the mixture was transferred and diluted in a centrifuge tube containing 1400 μL of pure water. The solution was mixed and cooled to 25 °C. The mixture (200 μL) was finally transferred into a 96-well microplate to record the absorbance at 540 nm. The results were expressed as the IC_{50} value (μg mL^{-1}). The inhibitory activity of the samples was compared with the standard drug acarbose, tested at identical concentrations of 0, 20, 40, 60, 80, and 100 μg mL^{-1}.

$$\text{α-Amylase inhibitory activity (\%)} = \frac{(\text{absorbance of control} - \text{absorbance of sample})}{\text{absorbance of control}} \times 100$$

2.12. α-Glucosidase inhibitory activity

All the solutions were prepared in phosphate buffer (0.1 M, pH 6.8). α-Glucosidase and PNPG were dissolved at 0.2 U mL^{-1} and 2.5 mM concentrations, respectively. 8 μL of the sample (250–1000 μg mL^{-1}), followed by 112 μL of the buffer and 20 μL of α-glucosidase solution, was transferred to a 96-well microplate and left for incubation for 15 min at 37 °C. The 20 μL of PNPG solution was added, followed by 15 min incubation at 37 °C. Finally, 80 μL of 0.2 M Na_2CO_3 solution was added to terminate the reaction.

The absorbance was measured at 405 nm. The α-glucosidase inhibitory activity was expressed as the IC_{50} value (μg mL^{-1}).

$$\alpha\text{-Glucosidase inhibitory activity (\%)} = \frac{(\text{absorbance of control} - \text{absorbance of sample})}{\text{absorbance of control}} \times 100$$

The IC_{50} values for α-amylase and α-glucosidase inhibition were also determined using *GraphPad Prism* software. The percentage inhibition data obtained at 5 different sample concentrations were plotted against the logarithm of concentration, and a non-linear regression analysis was performed using a four-parameter logistic (4PL) dose–response model. The concentration corresponding to 50% inhibition (IC_{50}) and its 95% confidence interval were automatically generated by the software. All measurements were carried out in triplicate, and the mean IC_{50} values were reported.

2.13. Experimental design and statistical analysis for SFE

In the present research, pressure, temperature, and extraction time in RSM were three independent variables designed to optimize TPC (mg per g of DWB) from *LS* leaves. Meanwhile, the CO_2 flow rate and particle size were kept constant throughout the experiments. The independent parameters X_1, X_2 and X_3 represent the leaves' pressure, temperature and extraction time, respectively. These parameters reflect the three coded levels of −1, 0 and +1 for a pressure of 20, 30 and 40 MPa; a temperature of 70, 90 and 110 °C; and an extraction time of 30, 50 and 70 min (Table 1). In RSM, Central Composite Design (CCD) is used as an experimental technique to create model equations. Eight factorials, six axials, and six central points were the combinations of three different parameters that CCD suggested in 20 trials. Six repeats of the centre point were conducted to determine the method's repeatability test. The RSM design and analysis were performed using *Design Expert* 13.0.5.0 (Stat-Ease Inc., Minneapolis, USA) to optimise the total phenolic content.

Regression analysis was used to examine the actual experiment findings and determine the effectiveness of several numerical models for statistically describing the yield of TPC. The analysis of variance (ANOVA) was used to examine the regression components of these various models and how they affected the optimisation outcomes. The generated equation's mathematical relevance was demonstrated using the determination coefficient (R^2), adjusted determination coefficient (adj. R^2), anticipated determination coefficient (pred. R^2), and lack-of-fit. The values of $p < 0.05$ were considered significant. A three-dimensional (3D) response surface map based on the chosen statistical model was created to analyze the linear and interaction terms of the independent factors on the response. The absolute optimal conditions of process parameters to create desired response ranges were predicted using mathematical optimization techniques. To confirm the effectiveness of the regression model, experimental data were compared with the values predicted by the model.

3 Results and discussion

3.1. Optimization of SFE parameters and model analysis

A 96.65% significant quadratic model was found among the suggested statistical models, which would predict and optimize the yield of TPC. Statistical analysis of regression coefficients concluded that the total extraction yield of TPC depends linearly on extraction pressure (X_1), temperature (X_2) and extraction time (X_3). The interaction between pressure–temperature (X_1X_2), pressure–extraction time (X_1X_3) and temperature–extraction time (X_2X_3) provides an idea about the process economics. Furthermore, significant terms of the model include quadratic terms of pressure (X_1^2) and temperature (X_2^2). It was regarded that there was no statistically significant interaction between the independent variables under study and the quadratic term of extraction time (X_3^2). The final response of the TPC quadratic regression model is given as:

$$\begin{aligned}\text{TPC (mg per g DWB)} = {} & +102.57 - 1.01X_1 - 0.0683X_2 + 1.64X_3 \\ & - 1.30X_1X_2 - 0.9250X_1X_3 \\ & - 0.5250X_2X_3 - 14.12X_1^2 - 2.25X_2^2 \\ & - 4.40X_3^2\end{aligned}$$

ANOVA was used to evaluate the model's integrity. A fitted quadratic model's ANOVA findings met the *F*-test confidence level. The *f*-value of the model was found to be 175.30. The *p*-value less than 0.0001 shows the excellent fit of a quadratic model. Meanwhile, the *p*-value of the "lack of fit" is 0.9795, suggesting a non-significant lack of fit, which is suitable for model fitting (Table 2). The interaction terms X_1X_2,X_1X_3, and X_2X_3 influence TPC yield. The correlation coefficient, "R^2", adjusted "R^2", and predicted "R^2" for a quadratic model of TPC yield are 0.9795, 0.9880 and 0.9865, respectively. Therefore, a statistical multiple regression relationship between the independent variables (pressure, temperature and extraction time) for the response TPC yield can be applied to predict the maximum extraction yield. Fig. 2 demonstrates a poor goodness-of-fit between the predicted values and the experimental data. Additionally, the coefficient of variance indicated low confidence in the model's performance. Among the variables, pressure had the most significant influence on the model.

3.2. Response surface analysis

Plots of two-factor interaction, as shown in Fig. 3a–c, were used to evaluate the effect of the interaction of differential parameters, pressure (a), temperature (b), and extraction time (c), on TPC yield from dried powder of *LS* leaves. The overall extraction yield was almost similar at 1% (100 mg) in all the experiments.

3.2.1. The effect of temperature and pressure on TPC yield. The extraction parameters in supercritical CO_2 extraction play a critical role in determining both the phenolic composition and biological activity of plant extracts. The 3D plot and contour plot in Fig. 3a show the effect of temperature and pressure on the maximum TPC yield at 90 °C and 30 MPa pressure. The results are tabulated in Table 3. The TPC yield decreases with

Table 2 Regression coefficients of the final regression model and ANOVA for the extraction yield in the CCD-PC design

Source	Sum of squares	d*f*	Mean square	*F*-Value	*p*-Value	
Model	3082.01	9	342.45	175.30	<0.0001	Significant
X_1	13.86	1	13.86	7.10	0.0237	
X_2	0.0636	1	0.0636	0.0326	0.8604	
X_3	36.87	1	36.87	18.88	0.0015	
X_1X_2	13.52	1	13.52	6.92	0.0251	
X_1X_3	6.85	1	6.85	3.50	0.0907	
X_2X_3	2.20	1	2.20	1.13	0.3130	
X_1^2	2873.14	1	2873.14	1470.77	<0.0001	
X_2^2	73.13	1	73.13	37.44	0.0001	
X_3^2	278.63	1	278.63	142.63	<0.0001	
Residual	19.53	10	1.95			
Lack of fit	2.21	5	0.4413	0.1273	0.9795	Not significant
Pure error	17.33	5	3.47			
Cor total	3101.55	19				

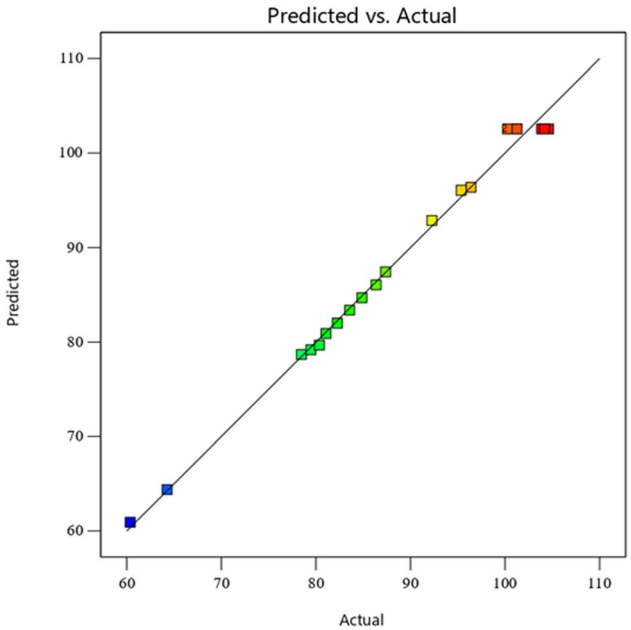

Fig. 2 The correlation between the actual experimental values and the model's predicted values for total polyphenolic content.

pressure fluctuations above and below 30 MPa. This is due to pressure and temperature that directly influence the solvent density and diffusivity, which in turn affect the solubility of polar and semi-polar phenolic compounds in CO_2.[17] Although pressure is the primary extraction parameter, it significantly affects the TPC yield.[18] The yield of TPC was maximum at a pressure of 30 MPa and was nearly the same when a pressure of 30 MPa was applied with variable time. However, a reduced extraction yield was found when the temperature was kept at more and less than 90 °C at the same pressure. The present results showed similar observations with Piper Betel Linn leaves' phenolic content, which depicts the higher extraction yield when 30 MPa pressure was applied at 80 °C temperature.[19]

At a certain level, high pressure reduces the density of SC-CO_2 to minimize the interaction with the sample and lowers the mass transfer during extraction. Furthermore, the moderate pressures (30 MPa), CO_2 attains sufficient density to dissolve low- to medium-polar phenolics such as vanillic acid and vanillin.[20]

In agreement with the previous study, the author stated that high pressure reduces the diffusion rates of solutes, which may be the case with the supercritical fluid medium. Hence, with pressure higher than 30 MPa, less extraction efficacy was obtained than expected due to the key role of diffusion in the mass transfer rates of the extractable materials from the sample matrix into the supercritical fluid environment.[21] Based on the optimal condition when we analyze pressure in statistics, the highest TPC yield was obtained at 29.59 MPa.

The temperature did not show a higher impact on TPC yield than pressure, though its impact on extraction is more challenging to explain due to its 2 reverse effects. First, its higher temperature lowers the SC-CO_2 density, and second, its high temperature accelerates the solubility of the compound in SC-CO_2 and enhances the extraction yield.[22,23] The interaction between SC-CO_2 and dried powdered matrix decreased with an increased temperature of 90 °C. The balance between these opposing effects consequently established the optimal temperature condition is 89.50 °C, as suggested by statistical analysis.

The CO_2 flow rate, though constant in this study, also governs solute transport and residence time in the extraction vessel, influencing selectivity and yield.[17] Variations in these parameters can therefore alter the relative abundance of individual phenolic acids, which ultimately affects antioxidant and enzyme inhibitory properties. Previous studies have shown that phenolic acids such as *p*-hydroxybenzoic acid and vanillin exhibit enhanced recovery and activity under optimized supercritical conditions due to minimized thermal degradation and oxidation.[19,24] Hence, the strong bioactivity observed under our optimized conditions can be attributed to the favorable solubility diffusion balance achieved by the selected pressure–temperature combination.

3.2.2. Effect of extraction time on TPC yield. The interaction of extraction time–temperature and extraction time–

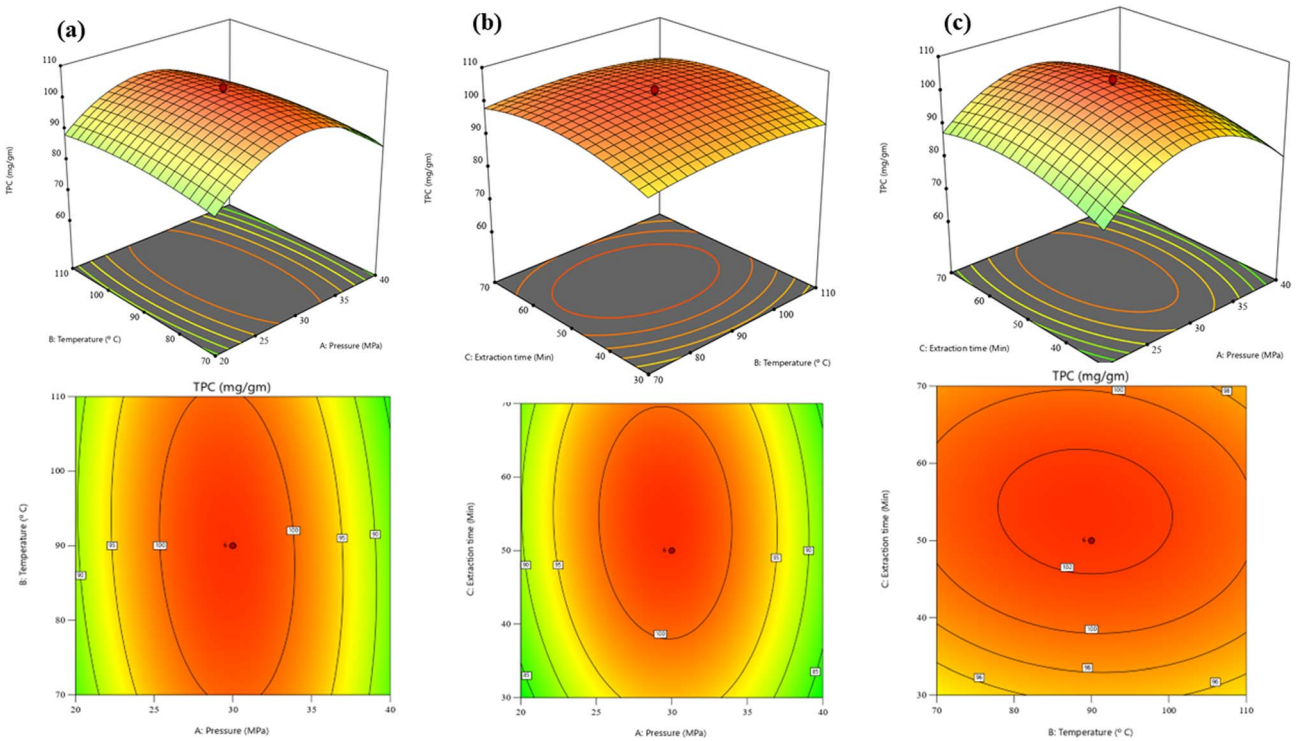

Fig. 3 The response surface plot shows the effect of two SC-CO_2 parameters on total phenolic content yield (mg per g of DWB): (a) total phenolic content yield *vs.* extraction temperature and pressure with a constant extraction time of 50 min, (b) total phenolic content yield *vs.* extraction time and temperature with a constant pressure of 30 MPa, and (c) total phenolic content yield *vs.* extraction time and pressure with a constant temperature of 90 °C.

pressure is shown in Fig. 3b and c. The contour plot showed that the extraction was carried out at constant temperature and pressure with varied extraction times ranging from 30 to 70 min. A pressure of 30 MPa shows a high density of SC-CO_2, which results in a higher extraction yield.[25] That could be one of the reasons that time did not alter much of the extraction yield. However, the maximum extraction yield of 104.67 mg per g of DWB was reduced to 92.27 mg per g TPC of DWB with the increase in time from 50 to 83.63 min. As the extraction was carried out in static mode, the thermolabile components must be degraded at a higher temperature when kept in a more extended static mode. The optimal extraction time was determined to be 53.85 min, yielding 99.31 ± 2.57 TPC mg per g of DWB. SFE-*LS* yielded a higher concentration of phenolic content than standardized leaf extract from Changsha Botaniex Inc, China (72.3 ± 0.293 mg per mL GAE per 100 g).[26]

3.2.3. Determination of the optimum conditions. A pressure of 29.59 MPa, a temperature of 89.50 °C and an extraction time of 53.85 min are the optimum parameters for the maximum extraction of phenolic content from *LS*. Under these parameters, the predicted value of *LS*-TPC was 102.749 mg per g of DWB. The experiments were conducted to verify the expected value of 99.31 ± 2.57 mg per g of DWB, similar to the predicted one. The closeness between predicted (102.749 mg per g of DWB) and experimental (99.31 ± 2.57 mg per g of DWB) values justified the efficacy of the response surface model established to understand the influence of independent parameters for maximum yield of *LS*-TPC using SFE.

3.3. Effect of high-pressure extraction on biomass

FE-SEM was performed to explain the effect of high-pressure SC-CO_2 on the physical structure of leaf biomass (Fig. 4). Due to the high extraction pressure, the solvent reached the cellular biomass and penetrated the cell. A study has shown that a temperature increase reduces the solvent's density and viscosity, allowing cavitation bubbles to develop in the extraction medium. The process of cavitation bubble generation and collapse results in deep penetration of the solvent into the cell matrix and increases the mass transfer rate.[27] Since a particle size of less than 500 μm was used in every experiment, there were no uniform particles. Establishing a consistent magnification factor was challenging, making it impossible to compare the particles before and after extraction. The surface of the leaves was found to have a shrunken physical structure with multiple stomatal openings, Fig. 4b indicates the extraction of inner material from the cell. Fig. 4a shows fewer stomatal apertures because no pressure was applied to the leaf biomass. The targeted phenolic compounds occur in bounded forms in intercellular vacuoles.[28] Once the solvent reached the cellular components during the extraction procedure, molecular diffusion occurred.

Based on the optimized extraction parameters (29.59 MPa, 89.50 °C, and 53.85 min), the phenolic composition of the supercritical CO_2 extract was subsequently examined to identify the major bioactive constituents responsible for its functional properties. This analysis was crucial to establish a link between extraction efficiency and the chemical nature of the recovered phenolics.

Table 3 Central composite design matrix of independent parameters for TPC yield (mg per g DWB) with actual experimental and predicted values[a]

		Independent parameters						Total phenolic content (mg per g DWB)	
		Pressure		Temperature		Extraction time			
No.	Point type	X_1	P (bar)	X_2	T (°C)	X_3	ET (min)	Experimental	Predicted
1	Factorial	−1	20	−1	70	−1	30	78.17	78.48
2	Factorial	+1	40	−1	70	−1	30	81.07	80.92
3	Factorial	+1	40	−1	70	+1	70	83.57	83.40
4	Factorial	+1	40	+1	110	−1	30	79.47	79.23
5	Factorial	+1	40	+1	110	+1	70	80.37	79.62
6	Factorial	−1	20	+1	110	+1	70	86.37	86.08
7	Factorial	−1	20	−1	70	+1	70	84.87	84.67
8	Factorial	−1	20	+1	110	−1	30	82.27	82
9	Axial	0	30	−2	56.36	0	50	96.4	96.31
10	Axial	+2	46.81	0	90	0	50	60.37	60.94
11	Axial	0	30	0	90	+2	83.63	92.27	92.90
12	Axial	−2	13.18	0	90	0	50	64.27	64.33
13	Axial	0	30	0	90	−2	16.36	87.37	87.37
14	Axial	0	30	+2	123.63	0	50	95.37	96.08
15	Central	0	30	0	90	0	50	104.17	102.57
16	Central	0	30	0	90	0	50	104.67	102.57
17	Central	0	30	0	90	0	50	101.27	102.57
18	Central	0	30	0	90	0	50	103.87	102.57
19	Central	0	30	0	90	0	50	100.27	102.57
20	Central	0	30	0	90	0	50	101.27	102.57

[a] X_1: pressure; X_2: temperature; X_3: extraction time; −1: low level; 0: medium level; +1: max level; −2: lower than experimental range level; +2: higher than experimental range level.

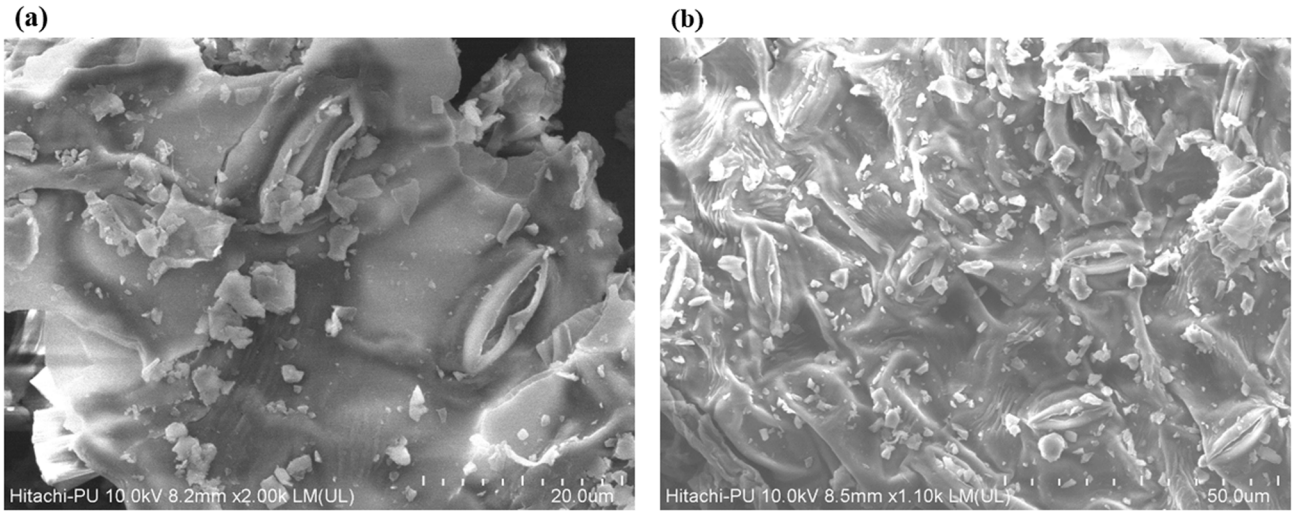

Fig. 4 FESEM image of *LS* powder: (a) before extraction and (b) after extraction.

3.4. Identification and quantification of phenolic compounds in SFE-*LS* extract

Optimized SFE-*LS* extract was analysed for seven phenolic compounds *viz* benzoic acid, *p*-hydroxybenzoic acid, chlorogenic acid, vanillic acid, vanillin, syringic acid and *p*-coumaric acid. The linearity for the compounds was assessed at eight-point concentration levels (5–500 μg mL^{-1}) except benzoic acid, which was evaluated at a 5-point concentration level (100–500 μg mL^{-1}). The calibration curve was prepared between the peak area and the concentration range. The curves were linear with the linear equation as the value of Y, and the correlation coefficient R^2 showed good linearity for all the compounds with a high correlation degree. The p-value < 0.05 showed statistically significant results. The data, when compared to the standard chromatogram (Fig. 5a), revealed that *p*-hydroxybenzoic acid

contents (91.88 ± 12.39 μg per g of DWB) were highest, followed by those of vanillic acid (77.47 ± 3.55 μg per g of DWB), *p*-coumaric acid (52.92 ± 3.13 μg per g of DWB), chlorogenic acid (42.41 ± 1.04 μg per g of DWB) and vanillin (31.82 ± 1.95 μg per g of DWB) (Fig. 5b). Recently, it has been investigated that these hydroxybenzoic acids are essential bioactive compounds in terms of their antioxidant and antidiabetic potential.[29,30] This could be one of the reasons that SFE-*LS* showed significant biological activity. Notably, *LS* is a good source of these essential bioactive polyphenols, and CO_2 is an effective solvent for recovering considerable quantities of these polyphenols. Vanillic acid, *p*-coumaric acid, chlorogenic acid, and vanillin are phenolic compounds that are conservative in various plants and also show diverse pharmacological activities.[31,32] Alkyl esters of *p*-hydroxybenzoic acid are frequently used as antibacterial agents in foods, cosmetics, toiletries, and medications. According to reports, they exhibit various antimicrobial effects, including fungicidal effects.[33] SFE-*LS* obtained using our designed experiments showed significant antiradical and even *in vitro* antidiabetic activity. This indicates that the extracts of *LS* leaves through SFE have better functional quality due to high-quality phenolic compounds. Finally, it should be

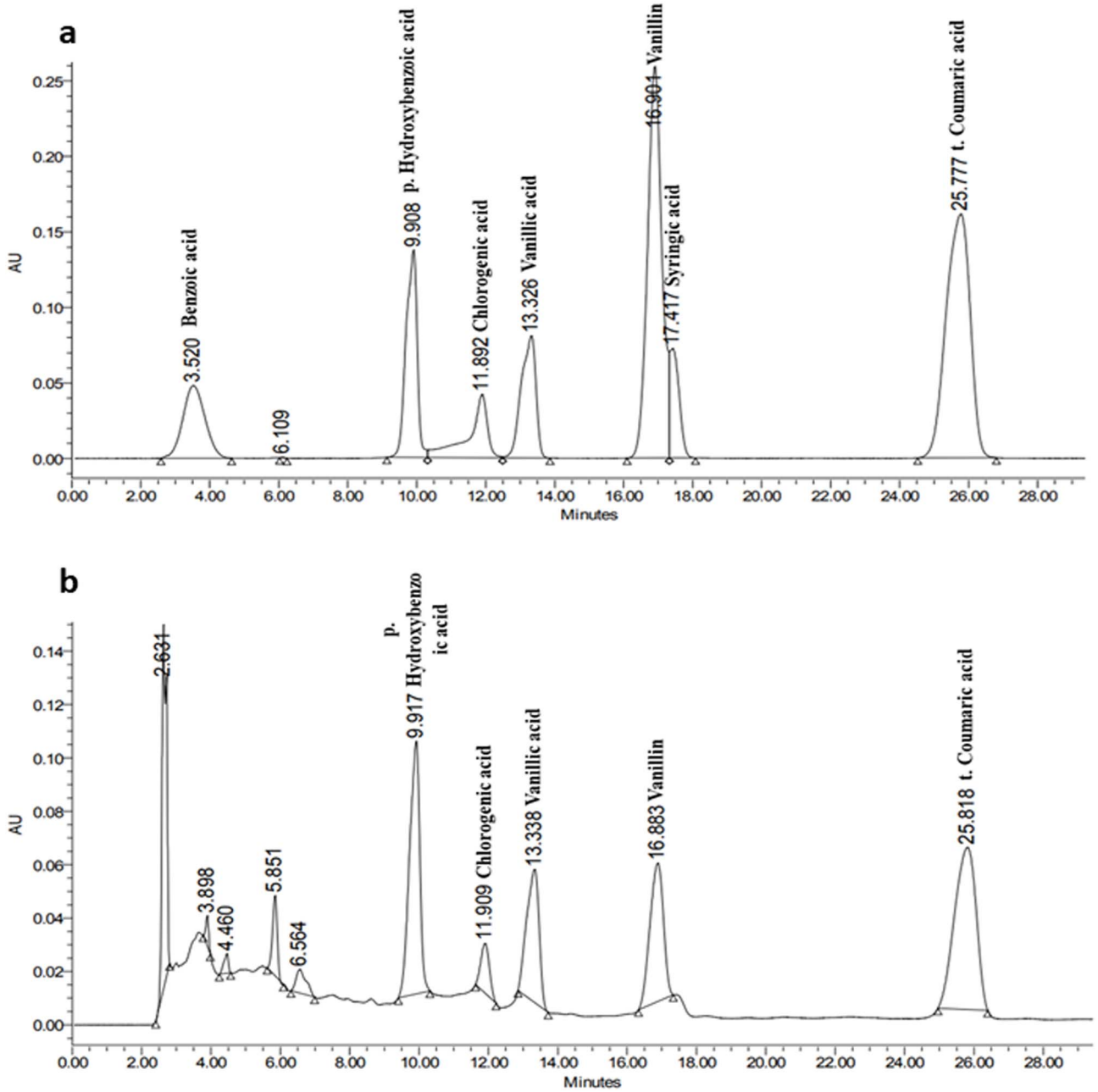

Fig. 5 (a) UPLC-chromatogram of phenolic standards: benzoic acid, hydroxybenzoic acid, chlorogenic acid, vanillic acid, vanillin, syringic acid, and *p*-coumaric acid. (b) Determination of phenolic compounds in SFE-*LS* optimized extract.

accentuated that the supercritical CO_2 extracted phenolic composition of *LS* leaves analysed by UPLC is published here for the first time. Among the identified compounds, vanillin and *p*-coumaric acid were found in considerable amounts and are well-known for their biological activities. Therefore, these phenolics were selectively purified from the optimized extract to obtain higher purity fractions for structural characterization and bioactivity assessment.

3.5. Purification of vanillin and *p*-coumaric acid using column chromatography

After optimization of extraction, phenolic compounds were further purified *via* adsorption through Diaion HP-20 adsorbent resin. In this step, vanillin and *p*-coumaric acid were separated from other compounds. Diaion HP-20 resin is a polystyrene/divinylbenzene matrix selected to exploit π–π interactions for aromatic compounds. Due to the aromatic reversed-phase adsorbent nature of the resin, the purification was carried out using an increased proportion of methanol to water to purify vanillin and *p*-coumaric acid. The obtained fractions were subjected to UPLC-PDA analysis to quantify the compounds obtained. Vanillin and *p*-coumaric acid showed increased desorption from resin as the methanol concentration was increased from 50% to 70%. Vanillin and *p*-coumaric acid were detected in both the fractions of 70% methanol and 90% methanol. This could be possible because of the small size difference, which is 168.14 g mol^{-1} and 164.16 g mol^{-1} for vanillin and *p*-coumaric acid, respectively.[34] Fraction 22 eluted with 70% methanol showed 4 compounds significantly, including *p*-hydroxybenzoic acid, vanillic acid, vanillin and *p*-coumaric acid, as shown in Fig. 6a. Elution of vanillin and *p*-coumaric acid alone was seen with additional purification using the increased methanol concentration to 90%, which was confirmed in fraction 26 by UPLC (Fig. 6b). These results suggest that the highest purity of vanillin and *p*-coumaric acid can be achieved in 90% methanol, suggesting this solvent mixture is more suitable for the desorption of vanillin and *p*-coumaric acid. The concentration detected was 32.65 μg mL^{-1} and 27.65 μg mL^{-1} for *p*-coumaric acid and vanillin, respectively. Fraction 29, purified with 90% methanol, yielded purified vanillin (376.23 μg mL^{-1}), and fraction 30 yielded purified *p*-coumaric acid (393.25 μg mL^{-1}), as shown in Fig. 6c and d, respectively. The fractions were dried *in vacuo* and used for NMR analysis. These fractions are referred to as HP-20 purified fractions.

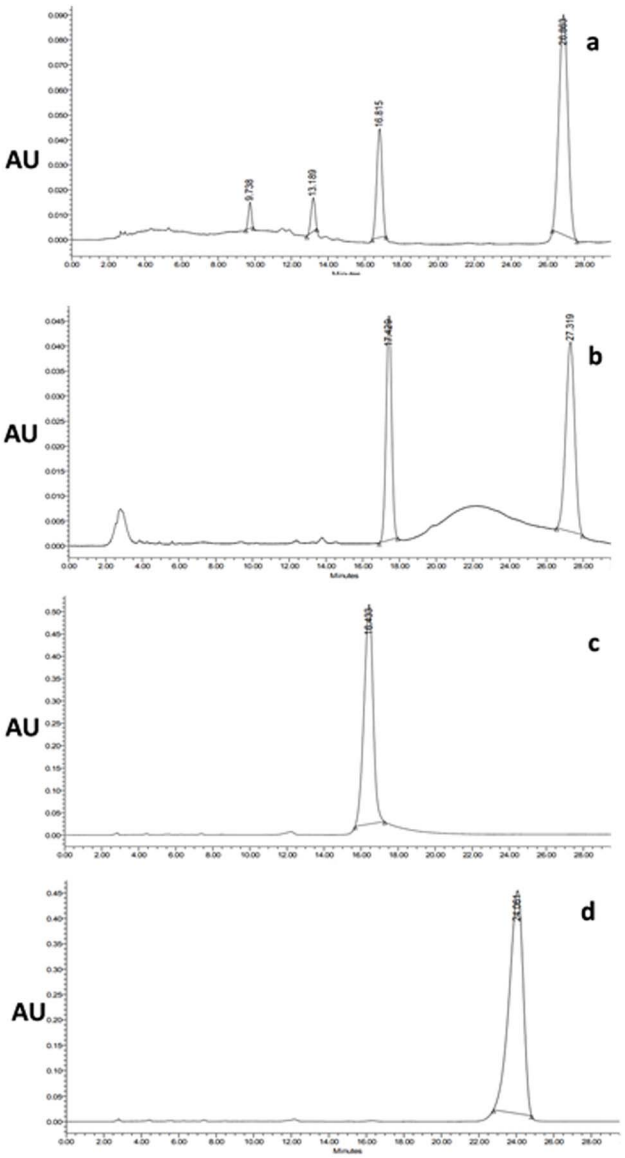

Fig. 6 Purification of vanillin and *p*-coumaric acid using DIAION HP-20 column chromatography: fraction 22 (a), fraction 26 (b), fraction 29 (c), and fraction 30 (d).

3.6. Identification of compounds in purified fractions

The chemical structure of vanillin and *p*-coumaric acid was analyzed using ^{1}H NMR (Fig. 7a and b). The ^{1}H NMR spectrum showed the presence of prominent peaks around $\delta = 3.74$, 6.9, 7.230, 7.233 and 9.44 ppm, corresponding to methyl ($-CH_3$), hydrogen ($-H_4$), (H_2), (H_3) and ($-H_1$) groups, respectively (Fig. 7a), confirming the presence of vanillin in the fraction.[35] Fig. 7b shows the ^{1}H NMR spectrum of *trans*-*p*-coumaric acid and the assignments of its protons. The scalar coupling constant of the trans protons of the vinyl double bond H_1–H_2 is present at chemical shifts of δ 6.437 and 7.69, respectively. Along with these, the presence of H_3 and H_4 groups at δ 6.9 and 7.6 confirms the intimacy of *p*-coumaric acid. Our results agree with the research of Kort *et al.*[36] After confirming the structure and purity of vanillin and *p*-coumaric acid through NMR analysis, the biological potential of both the crude SFE extract and the purified fractions was evaluated. This allowed us to investigate how the identified phenolic profile translated into measurable antioxidant and enzyme inhibitory activities.

3.7. Evaluation of *in vitro* antidiabetic and antioxidant activity

3.7.1. α-Glucosidase inhibitory activity by SFE-*LS* extract, purified vanillin and purified *p*-coumaric acid. One of the most effective ways to reduce postprandial hyperglycemia is to reduce

Fig. 7 (a) ^{1}H NMR for fraction 29 (vanillin) and (b) ^{1}H NMR for fraction 31 (*p*-coumaric acid).

glucose synthesis and/or absorption from the gastrointestinal tract by inhibiting the activity of the two main digestive enzymes, α-glucosidase and α-amylase. α-Glucosidase, the enzyme at the mucosal brush border, is a carbohydrate-hydrolyzing enzyme that breaks down α-glycosidic bonds in di, tri and oligosaccharides to synthesize glucose and other absorbable monosaccharides. The prevention of high post-prandial blood glucose levels and the delay of glucose absorption can be achieved by its suppression, which may likely slow the course of diabetes.[37,38]

The results of α-glucosidase inhibition of SFE-*LS* crude extract are presented in Table 4. The extract showed significant (IC_{50} 59.45 ± 3.4) ($p < 0.05$) α-glucosidase inhibitory activity. Interestingly, the extract showed a comparable inhibitory effect with the commercially available drug acarbose (IC_{50} 23.58 ± 2.1) ($p < 0.05$). The results are shown in Fig. 8a and b. The inhibitory activity against the enzyme may result not only from the overall polyphenolic content but also specifically from the phenolic acids such as vanillic acid, *p*-coumaric acid, and chlorogenic acid, which are known to interact with the catalytic residues of α-amylase and α-glucosidase through hydrogen bonding and hydrophobic interactions.[39] Although the variation in effectiveness depends on the difference in their structure, their mode of action and binding ability to the inhibitory site also influence their effectiveness.[40] To clarify this, we further studied the effect of purified compounds on enzyme inhibition for better results.

Meanwhile, a considerable glucosidase inhibitory activity was seen in vanillin purified fraction (IC_{50} 31.90 ± 1.96 μg mL^{-1}) ($p < 0.05$). Vanillin demonstrated the most active inhibition against α-glucosidase, comparable to acarbose ($p < 0.05$). The primary interaction between the enzyme and the inhibitors during enzyme inhibition is hydrophobic.[41] The inhibition by vanillin was found to be the most effective among all tested samples, and this observation is supported by the findings of Liu *et al.* (2021), who confirmed through molecular docking that vanillin interacts with α-glucosidase *via* hydrophobic and hydrogen-bonding interactions (−8.42 kcal mol^{-1} binding energy), causing steric hindrance at the active site of the enzyme.[42]

This study showed better α-glucosidase inhibitory activity than previously published data.[43] The inhibition of α-glucosidase remains one of the potential activities of the SFE-*LS* extract and its purified fractions. The *p*-coumaric acid fraction showed the lowest inhibition of α-glucosidase (IC_{50} 88.32 ± 5.64 μg mL^{-1}) ($p < 0.05$) as compared to other samples. *p*-Coumaric acid itself does not show effective inhibition against the α-glucosidase or α-amylase, but in combination with ferulic acid and chlorogenic acid, it completely inhibits the enzyme.[44]

Table 4 IC_{50} values for α-glucosidase and α-amylase inhibition by SFE-*LS* extract and acarbose

		IC_{50} value (μg mL^{-1})	
Sr. No.	Sample name	α-Amylase inhibition	α-Glucosidase inhibition
1	SFE-*LS*	30.09 ± 2.58	59.45 ± 3.4
2	Vanillin	22.91 ± 0.5	31.90 ± 1.96
3	*p*-Coumaric acid	71.87 ± 6.2	88.32 ± 5.64
4	Acarbose	20.97 ± 0.86	23.58 ± 2.1

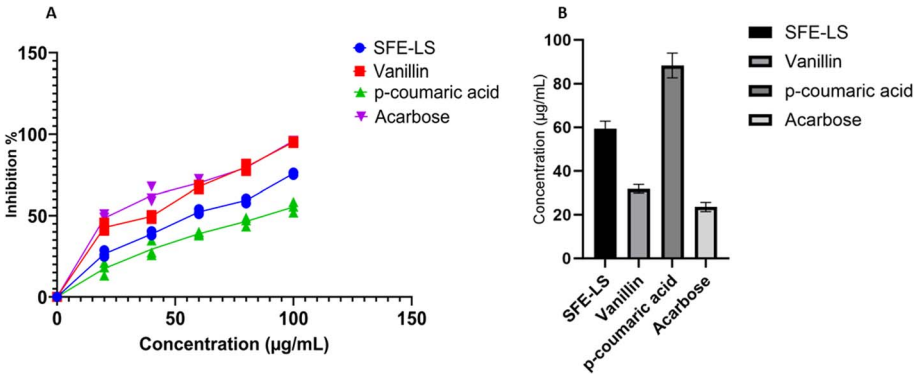

Fig. 8 Alpha glucosidase inhibition by SFE-*LS* extract, vanillin, *p*-coumaric acid, and acarbose: dose-dependent inhibition (A) and IC_{50} calculation for the inhibition of alpha glucosidase (B).

The findings indicated that SFE and HP-20 purified fractions have an inhibitory effect comparable to other natural substances, suggesting that they can be used as a natural α-glucosidases inhibitor for inclusion in dietary foods.

3.7.2. α-Amylase inhibitory activity by SFE-*LS* extract, purified vanillin and purified *p*-coumaric acid. α-Amylase is a vital enzyme in saliva and pancreatic juice, secreted by the salivary glands and pancreas.[45] The polysaccharide breakdown from complex dietary sugar into disaccharides begins in the mouth before being further broken down in the small intestine by other intestinal enzymes.[46] Inhibiting the major enzymes associated with hyperglycemia through food management may be a novel and complete nutritional approach for the reduction of postprandial blood glucose levels.[47,48]

α-Amylase inhibitory activity of SFE-*LS* extract is shown in Fig. 9a and b. The results were in agreement with the α-glucosidase inhibition. The maximum α-amylase inhibitory effect was observed in the vanillin fraction (IC_{50} 22.91 ± 0.5 μg mL^{-1}), which was approximately near the standard drug acarbose (IC_{50} 20.97 ± 0.86 μg mL^{-1}) ($p < 0.05$). The crude SFE-*LS* even showed significant inhibitory activity against α-amylase (IC_{50} 30.09 ± 2.58 μg mL^{-1}) ($p < 0.05$), followed by *p*-coumaric acid (IC_{50} 71.87 ± 6.2 μg mL^{-1}). This suggests that the inhibition of amylase is more dependent on the structure of vanillin, which gives better purification results than crude extract. These results are supported by similar findings that vanillin was the most active α-amylase inhibitor and that *p*-coumaric acid is a moderate inhibitor.[44,49] In fact, numerous studies have documented the advantages of phenolics as α-amylase and α-glucosidase inhibitors.[50] Previous reports suggested that phenolic compounds bind to the catalytic site of α-amylase and inhibit its reaction.[51] The report suggested that SFE-*LS* and purified fractions lower glucose levels more effectively by inhibiting α-amylase rather than α-glucosidase.

Overall, these results demonstrated that vanillin from *LS* exhibits a notably stronger inhibitory effect than most reported phenolic acids, while *p*-coumaric acid remains within the moderate range of inhibition previously observed for natural polyphenols. The observed enzyme inhibitory potential also correlates with the high TPC of the extract, suggesting that both the quantity and the structural diversity of phenolic constituents contribute collectively to the α-amylase inhibitory activity.

Some plants traditionally used in diabetes management were found to strongly inhibit α-glucosidase but had a moderate or negligible effect on α-amylase activity.[52] α-Glucosidase inhibitors have gained more attention in recent studies than α-amylase inhibitors. These inhibitors are considered promising alternatives to synthetic enzyme inhibitors such as acarbose.[53] The American Association of Clinical Endocrinologists (AACE) and the International Diabetes Federation (IDF) have recommended α-glucosidase inhibitors as a first-line therapy for managing diabetes due to their efficacy.[54] Because oxidative

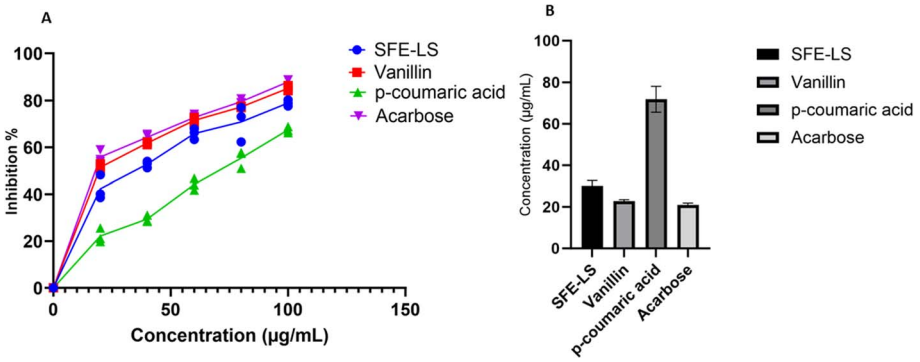

Fig. 9 Alpha amylase inhibition by SFE-*LS* extract, vanillin, *p*-coumaric acid, and acarbose: dose-dependent inhibition (A) and IC_{50} calculation for the inhibition of alpha amylase (B).

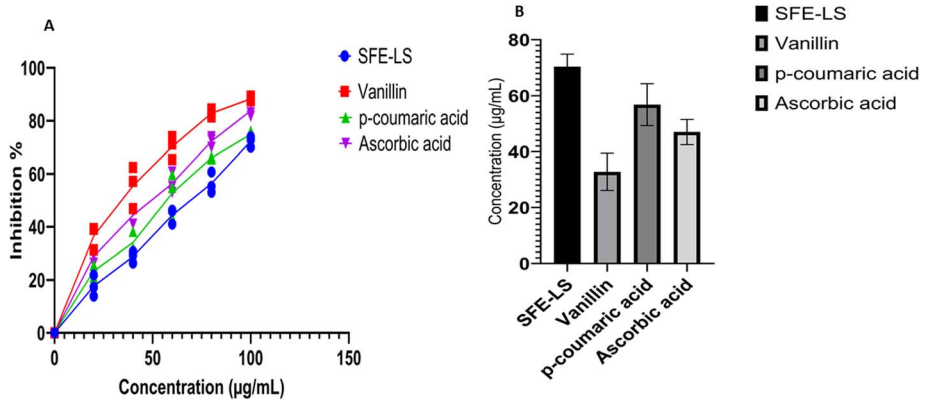

Fig. 10 Antioxidant activity of SFE-*LS* extract, vanillin, *p*-coumaric acid, and ascorbic acid: dose-dependent inhibition of 2,2-diphenyl-1-picrylhydrazyl (A) and IC_{50} calculation for the inhibition of 2,2-diphenyl-1-picrylhydrazyl (B).

Table 5 IC_{50} values for DPPH radical scavenging activity of SFE-*LS* extract and ascorbic acid

Sr. No.	Sample name	IC_{50} value (µg mL^{-1}) DPPH radical scavenging activity
1	SFE-*LS*	70.43 ± 4.36
2	Vanillin	32.76 ± 6.6
3	*p*-Coumaric acid	56.80 ± 7.5
4	Ascorbic acid	46.96 ± 4.51

stress and carbohydrate metabolism are closely interconnected in diabetes pathophysiology, we further examined whether the antioxidant properties of the extract and purified phenolics complemented their enzyme inhibitory activities.

3.8. Evaluation of the antioxidant activity of SFE-*LS* extract, purified vanillin and purified *p*-coumaric acid

Plant phenolic compounds are widely recognized for their potent *in vitro* antioxidant activity due to their ability to donate electrons or hydrogen atoms and stabilize radical intermediates.[55] The DPPH radical scavenging activity of SFE-*LS* increased progressively with concentration (20–100 µg mL^{-1}), as shown in Fig. 10, indicating a clear dose-dependent response. The extract exhibited significant radical-quenching ability with an IC_{50} value of 70.43 ± 4.36 µg mL^{-1} ($p < 0.05$; Table 5).

Purified phenolic fractions showed enhanced activity compared with the crude extract. Among these, the vanillin-rich fraction demonstrated the strongest DPPH scavenging effect (IC_{50} = 32.76 ± 6.6 µg mL^{-1}), surpassing even the standard ascorbic acid, while *p*-coumaric acid (IC_{50} = 46.96 ± 4.51 µg mL^{-1}) exhibited comparable activity. Interestingly, our findings differ from those of ref. 56, which reported stronger activity of *p*-coumaric acid relative to vanillin in *Oryza sativa* extract. Such variations may arise from differences in plant matrix composition, phenolic concentration, or extraction technique, which can influence compound stability and synergistic interactions. The variations in species, cultivar, and geographical origin often lead to distinct phytochemical profiles and phenolic concentrations. Additionally, the use of SC-CO_2 extraction in the present study, unlike conventional solvent-based methods reported earlier, provides selective recovery of thermolabile and moderately polar phenolics while minimizing oxidative degradation, which may enhance apparent bioactivity. Matrix effects, such as particle size, moisture content, and cellular structure, can also influence mass transfer efficiency during extraction, thereby affecting yield and composition.

The radical-scavenging ability of phenolic compounds largely depends on their structural configuration, particularly the number and position of hydroxyl groups and other substituents on the aromatic ring.[57] The pronounced activity observed for the SFE-*LS* extract and vanillin fraction suggests that structural factors, along with possible synergistic effects among phenolic constituents, enhance the overall antioxidant capacity.[58,59] Thus, the antioxidant mechanism of the SFE-*LS* extract likely involves hydrogen- or electron-transfer processes that neutralize DPPH radicals and stabilize them into non-reactive species. Furthermore, the relationship between compound concentration and biological activity was observed qualitatively in the present study. The higher antioxidant and enzyme inhibitory activities correspond with elevated levels of vanillin and *p*-hydroxybenzoic acid identified in the SFE-*LS* extract. Both compounds are known for their strong reducing potential and effective radical-scavenging or enzyme-binding capabilities, which contribute to the overall bioactivity. The comparatively lower abundance of *p*-coumaric acid may explain its moderate antioxidant and inhibitory response. These results suggest a positive association between phenolic concentration and biological efficacy, consistent with earlier reports linking phenolic content with bioactivity in plant extracts.[20,24] Future studies employing quantitative correlation or regression analysis could further validate the contribution of individual

compounds to the overall antioxidant and antidiabetic effects of *LS* extracts. Although the present study employed only the DPPH radical-scavenging assay to evaluate antioxidant activity, it is nonetheless a widely accepted screening method for phenolic-rich extracts and has been shown in many studies to correlate with other antioxidant assays such as 2,2′-azino-bis (3-ethylbenzothiazoline-6-sulfonic acid) (ABTS) and ferric reducing antioxidant power (FRAP) under appropriate conditions. The findings of the current work of SFE-*LS* extract and its isolated fractions support meaningful radical-scavenging potential. Vanillin has been reported to show strong antioxidant behaviour in certain assays such as ABTS and oxygen radical absorbance capacity (ORAC), but negligible or weak activity in the DPPH assay because its mechanism includes self-dimerization or slower kinetics, which suggests that our positive DPPH result for vanillin is mechanistically plausible but should be interpreted with caution.[60] Conversely, *p*-coumaric acid exhibits consistent multi-assay antioxidant activity, including DPPH, ABTS, hydrogen peroxide scavenging, metal-chelation and reducing power, and thus our finding for the *p*-coumaric acid fraction aligns strongly with literature precedent.[61] Taken together, while the experimental limitation of having only one assay is noted, the combined evidence from our DPPH data, phenolic-compound identification and relevant literature supports the conclusion that the extract and its isolated fractions exhibit antioxidant potential. Future work could include complementary assays such as ABTS, FRAP, ORAC or cellular reactive oxygen species assays to further strengthen mechanistic insight.

4 Conclusion

This study successfully optimized SFE conditions for recovering TPC from *LS* leaves using RSM. The optimized parameters—29.59 MPa pressure, 89.50 °C temperature, and 53.85 min extraction time—resulted in high TPC yield, confirming the reliability of the developed model. The extract, rich in vanillic acid, *p*-hydroxybenzoic acid, chlorogenic acid, and vanillin, demonstrated strong antioxidant activity and significant inhibitory effects against key carbohydrate-hydrolysing enzymes, namely α-amylase and α-glucosidase, highlighting *LS* leaves as a promising natural source of bioactive compounds with potential antidiabetic properties. Despite these promising results, the present work is limited to *in vitro* studies and laboratory-scale extraction. Future research should include stability and safety assessments of the SFE-*LS* extract and its purified fractions under various storage and physiological conditions, along with formulation trials to develop functional food or nutraceutical products ensuring bioavailability and shelf stability. Moreover, the contradictions with some earlier literature may also stem from differences in assay conditions or enzyme sources used for inhibition studies. To confirm these hypotheses, future research should include comparative extraction studies using both supercritical and conventional methods, combined with metabolomic profiling to establish a comprehensive understanding of interspecies and matrix-dependent variability.

For real-world applications, challenges such as extract stability, large-scale process optimization, and regulatory compliance need to be addressed. Future studies should therefore focus on *in vivo* validation and toxicological assessments, and formulation trials aimed at developing functional food or nutraceutical products. Such efforts will support the translation of *LS* bioactive compounds from laboratory findings to practical health and industrial applications.

Author contributions

Kiran Khandare: investigation, experimental analysis, writing-original draft, manuscript editing and revision; Saswata Goswami: supervision, conceptualization, manuscript review and editing, resources, funding acquisition.

Conflicts of interest

The authors declare that they have no known competing financial or personal interests.

Abbreviations

AACE	American association of clinical endocrinologists
ANOVA	Analysis of variance
$AlCl_3$	Aluminium chloride
CAGR	Compound annual growth rate
CCD	Central composite design
CIAB	Center of innovative and applied bioprocessing
DMSO	Dimethyl sulfoxide
DPPH	2,2-Diphenyl-1-picrylhydrazyl
DWB	Dry weight of biomass
FE-SEM	Field emission scanning electron microscopy
GAE	Gallic acid equivalent
LOD	Limit of detection
LOQ	Limit of quantification
LS	*Lagerstroemia speciosa*
Na_2HPO_4	Sodium phosphate dibasic
NaH_2PO_4	Sodium phosphate monobasic
PDA	Photodiode array
PNPG	4-Nitrophenyl-β-D-glucopyranoside
RSM	Response surface methodology
SC-CO_2	Supercritical carbon-dioxide
SD	Standard deviation
SFE	Supercritical fluid extraction
TPC	Total phenolic content
UPLC-PDA	Ultra performance liquid chromatography coupled with photo diode array

Data availability

All data generated or analysed during this study are included in this research article and will be made available on request to corresponding author.

Acknowledgements

The authors are grateful for the research support received from the Center of Innovative and Applied Bioprocessing, Mohali. The authors also acknowledge Panjab University, Chandigarh and the Council of Scientific and Industrial Research, New Delhi.

References

1 T. Rohit Singh and D. Ezhilarasan, Ethanolic extract of Lagerstroemia Speciosa (L.) Pers., induces apoptosis and cell cycle arrest in HepG2 cells, *Nutr. Cancer*, 2020, **72**(1), 146–156.

2 M. P. Sonar and V. K. Rathod, Extraction of type ii antidiabetic compound corosolic acid from Lagerstroemia speciosa by batch extraction and three phase partitioning, *Biocatal. Agric. Biotechnol.*, 2020, **27**, 101694.

3 M. A. Al-Farsi and C. Y. Lee, Optimization of phenolics and dietary fibre extraction from date seeds, *Food Chem.*, 2008, **108**(3), 977–985.

4 M. Liza, R. A. Rahman, B. Mandana, S. Jinap, A. Rahmat, I. Zaidul, *et al.*, Supercritical carbon dioxide extraction of bioactive flavonoid from Strobilanthes crispus (Pecah Kaca), *Food Bioprod. Process.*, 2010, **88**(2–3), 319–326.

5 L. Mangiapelo, F. Blasi, F. Ianni, C. Suvieri, R. Sardella, C. Volpi, *et al.*, Optimization of a Simple Analytical Workflow to Characterize the Phenolic Fraction from Grape Pomace, *Food Bioprocess Technol.*, 2023, 1–16.

6 G. A. Martău, L.-F. Călinoiu and D. C. Vodnar, Bio-vanillin: Towards a sustainable industrial production, *Trends Food Sci. Technol.*, 2021, **109**, 579–592.

7 F. Liaqat, L. Xu, M. I. Khazi, S. Ali, M. U. Rahman and D. Zhu, Extraction, purification, and applications of vanillin: A review of recent advances and challenges, *Ind. Crops Prod.*, 2023, **204**, 117372.

8 S. Venkataraman, J. K. Athilakshmi, D. S. Rajendran, P. Bharathi and V. V. Kumar, A comprehensive review of eclectic approaches to the biological synthesis of vanillin and their application towards the food sector, *Food Sci. Biotechnol.*, 2024, **33**(5), 1019–1036.

9 E. Gomes and A. Rodrigues, Crystallization of vanillin from kraft lignin oxidation, *Sep. Purif. Technol.*, 2020, **247**, 116977.

10 S. Y. Ou, Y. L. Luo, C. H. Huang and M. Jackson, Production of coumaric acid from sugarcane bagasse, *Innovative Food Sci. Emerging Technol.*, 2009, **10**(2), 253–259.

11 S. Sansenya, A. Payaka and P. Mansalai, Biological activity and inhibition potential against α-glucosidase and α-amylase of 2, 4-di-tert-butylphenol from bamboo shoot extract by in vitro and in silico studies, *Process Biochem.*, 2023, **126**, 15–22.

12 S. Paul, A. Ali and R. Katare, Molecular complexities underlying the vascular complications of diabetes mellitus–A comprehensive review, *J. Diabetes Its Complications*, 2020, **34**(8), 107613.

13 A. P. Kalinovskii, O. V. Sintsova, I. N. Gladkikh and E. V. Leychenko, Natural inhibitors of mammalian α-amylases as promising drugs for the treatment of metabolic diseases, *Int. J. Mol. Sci.*, 2023, **24**(22), 16514.

14 P. Kolakul and B. Sripanidkulchai, Phytochemicals and anti-aging potentials of the extracts from Lagerstroemia speciosa and Lagerstroemia floribunda, *Ind. Crops Prod.*, 2017, **109**, 707–716.

15 R. Boran, Investigations of anti-aging potential of Hypericum origanifolium Willd. for skincare formulations, *Ind. Crops Prod.*, 2018, **118**, 290–295.

16 X.-F. Zhang, Y.-J. Tang, X.-X. Guan, X. Lu, J. Li, X.-L. Chen, *et al.*, Flavonoid constituents of Amomum tsao-ko Crevost et Lemarie and their antioxidant and antidiabetic effects in diabetic rats–in vitro and in vivo studies, *Food Funct.*, 2022, **13**(1), 437–450.

17 A. Molino, S. Mehariya, G. Di Sanzo, V. Larocca, M. Martino, G. P. Leone, *et al.*, Recent developments in supercritical fluid extraction of bioactive compounds from microalgae: Role of key parameters, technological achievements and challenges, *J. CO_2 Util.*, 2020, **36**, 196–209.

18 G. Herbst, F. Hamerski, M. Errico and M. L. Corazza, Pressurized liquid extraction of brewer's spent grain: Kinetics and crude extracts characterization, *J. Ind. Eng. Chem.*, 2021, **102**, 370–383.

19 Optimization of supercritical carbon dioxide extraction of Piper Betel Linn leaves oil and total phenolic content, *IOP Conference Series: Materials Science and Engineering*, ed. A. Aziz, M. Yunus, N. Arsad, N. Lee, Z. Idham and A. Razak, IOP Publishing, 2016.

20 T. Belwal, P. Dhyani, I. D. Bhatt, R. S. Rawal and V. Pande, Optimization extraction conditions for improving phenolic content and antioxidant activity in Berberis asiatica fruits using response surface methodology (RSM), *Food Chem.*, 2016, **207**, 115–124.

21 K. Rezaei and F. Temelli, Using supercritical fluid chromatography to determine diffusion coefficients of lipids in supercritical CO2, *J. Supercrit. Fluids*, 2000, **17**(1), 35–44.

22 G. Sodeifian, S. A. Sajadian and N. Saadati Ardestani, Evaluation of the response surface and hybrid artificial neural network-genetic algorithm methodologies to determine extraction yield of Ferulago angulata through supercritical fluid, *J. Taiwan Inst. Chem. Eng.*, 2016, **60**, 165–173.

23 L. Wang, X. Wang, P. Wang, Y. Xiao and Q. Liu, Optimization of supercritical carbon dioxide extraction, physicochemical and cytotoxicity properties of Gynostemma pentaphyllum seed oil: A potential source of conjugated linolenic acids, *Sep. Purif. Technol.*, 2016, **159**, 147–156.

24 H. S. Fathi, S. Lotfi, E. Rezvannejad, M. Mortazavi and A. Riahi-Madvar, Correlation between total phenolic and flavonoid contents and biological activities of 12 ethanolic extracts of Iranian propolis, *Food Sci. Nutr.*, 2023, **11**(7), 4308–4325.

25 S. Pourhoseini and A. Karimian, Optimization of oil extraction from Melia azedarach fruits using methanol-modified SC-CO2 for highly efficient biodiesel production using a modified LAC catalyst, *Fuel*, 2025, **380**, 133204.

26 S. M. Saumya, B. P. Mahaboob and P. Basha, In vitro evaluation of free radical scavenging activities of Panax ginseng and Lagerstroemia speciosa: a comparative analysis, *Int. J. Pharm. Pharm. Sci.*, 2011, **3**(1), 165–169.
27 P. C. Da, D. Decorti and A. Natolino, Application of a supercritical CO2 extraction procedure to recover volatile compounds and polyphenols from Rosa damascena, *Sep. Sci. Technol.*, 2015, **50**(8), 1175–1180.
28 R. J. Robbins, Phenolic Acids in Foods: An Overview of Analytical Methodology, *J. Agric. Food Chem.*, 2003, **51**(10), 2866–2887.
29 R. Farhoosh, S. Johnny, M. Asnaashari, N. Molaahmadibahraseman and A. Sharif, Structure–antioxidant activity relationships of o-hydroxyl, o-methoxy, and alkyl ester derivatives of p-hydroxybenzoic acid, *Food Chem.*, 2016, **194**, 128–134.
30 L. S. Tshane, S. S. Mashele, G. R. Matowane, S. L. Bonnet, T. J. Makhafola, A. E. M. Noreljaleel, *et al.*, Zinc (II) mineral increased the in vitro, cellular and ex vivo antihyperglycemic and antioxidative pharmacological profile of p-hydroxybenzoic acid upon complexation, *J. Food Biochem.*, 2021, **45**(2), e13609.
31 M. A. Yılmaz, P. Taslimi, Ö. Kılıç, İ. Gülçin, A. Dey and E. Bursal, Unravelling the phenolic compound reserves, antioxidant and enzyme inhibitory activities of an endemic plant species, Achillea pseudoaleppica, *J. Biomol. Struct. Dyn.*, 2023, **41**(2), 445–456.
32 F. Hadrich, M. Chamkha and S. Sayadi, Protective effect of olive leaves phenolic compounds against neurodegenerative disorders: Promising alternative for Alzheimer and Parkinson diseases modulation, *Food Chem. Toxicol.*, 2022, **159**, 112752.
33 S. Oishi, Lack of spermatotoxic effects of methyl and ethyl esters of p-hydroxybenzoic acid in rats, *Food Chem. Toxicol.*, 2004, **42**(11), 1845–1849.
34 F. Erpel, C. Camilo, R. Mateos and J. R. Pérez-Correa, A macroporous resin purification process to obtain food-grade phlorotannin-rich extracts with α-glucosidase inhibitory activity from Chilean brown seaweeds: an UHPLC-MSn profiling, *Food Chem.*, 2023, **402**, 134472.
35 ^{1}H NMR investigation of self-association of vanillin in aqueous solution, *Journal of Physics: Conference Series*, ed. M. Bogdan, C. G. Floare and A. Pîrnau, IOP Publishing, 2009.
36 R. Kort, H. Vonk, X. Xu, W. Hoff, W. Crielaard and K. Hellingwerf, Evidence for trans-cis isomerization of the p-coumaric acid chromophore as the photochemical basis of the photocycle of photoactive yellow protein, *FEBS Lett.*, 1996, **382**(1–2), 73–78.
37 H. Mechchate, I. Es-Safi, A. Louba, A. S. Alqahtani, F. A. Nasr, O. M. Noman, *et al.*, In vitro alpha-amylase and alpha-glucosidase inhibitory activity and in vivo antidiabetic activity of Withania frutescens L. Foliar extract, *Molecules*, 2021, **26**(2), 293.
38 U. Ghani, Re-exploring promising α-glucosidase inhibitors for potential development into oral anti-diabetic drugs: Finding needle in the haystack, *Eur. J. Med. Chem.*, 2015, **103**, 133–162.
39 M. A. H. Salahuddin, A. Ismail, N. K. Kassim, M. Hamid and M. S. M. Ali, Phenolic profiling and evaluation of in vitro antioxidant, α-glucosidase and α-amylase inhibitory activities of Lepisanthes fruticosa (Roxb) Leenh fruit extracts, *Food Chem.*, 2020, **331**, 127240.
40 G. Pan, Y. Lu, Z. Wei, Y. Li, L. Li and X. Pan, A review on the in vitro and in vivo screening of α-glucosidase inhibitors, *Heliyon*, 2024, **10**(18), e37467.
41 X. Du, Y. Li, Y.-L. Xia, S.-M. Ai, J. Liang, P. Sang, *et al.*, Insights into protein–ligand interactions: mechanisms, models, and methods, *Int. J. Mol. Sci.*, 2016, **17**(2), 144.
42 Y. Liu, J. Zhu, J. Yu, X. Chen, S. Zhang, Y. Cai, *et al.*, A new functionality study of vanillin as the inhibitor for α-glucosidase and its inhibition kinetic mechanism, *Food Chem.*, 2021, **353**, 129448.
43 B. T. D. Trinh, D. Staerk and A. K. Jäger, Screening for potential α-glucosidase and α-amylase inhibitory constituents from selected Vietnamese plants used to treat type 2 diabetes, *J. Ethnopharmacol.*, 2016, **186**, 189–195.
44 K. Pei, J. Ou, J. Huang and S. Ou, p-Coumaric acid and its conjugates: dietary sources, pharmacokinetic properties and biological activities, *J. Sci. Food Agric.*, 2016, **96**(9), 2952–2962.
45 B. R. Tonsic, V. G. Correa, J. A. A. Garcia-Manieri, A. Bracht and R. M. Peralta, An in vivo approach to the reported effects of phenolic acids and flavonoids on the pancreatic α-amylase activity, *Food Biosci.*, 2023, **51**, 102357.
46 M. Chakroun, B. Khemakhem, H. B. Mabrouk, H. El Abed, M. Makni, M. Bouaziz, *et al.*, Evaluation of anti-diabetic and anti-tumoral activities of bioactive compounds from Phoenix dactylifera L's leaf: In vitro and in vivo approach, *Biomed. Pharmacother.*, 2016, **84**, 415–422.
47 H. Patel, P. G. Royall, S. Gaisford, G. R. Williams, C. H. Edwards, F. J. Warren, *et al.*, Structural and enzyme kinetic studies of retrograded starch: Inhibition of α-amylase and consequences for intestinal digestion of starch, *Carbohydr. Polym.*, 2017, **164**, 154–161.
48 N. Kardum and M. Glibetic. Chapter Three - Polyphenols and Their Interactions With Other Dietary Compounds: Implications for Human Health, in *Advances in Food and Nutrition Research*, ed. F. Toldrá, Academic Press, vol. 84, 2018, pp. 103–44.
49 N. Laaraj, M. Bouhrim, L. Kharchoufa, S. Tiji, H. Bendaha, M. Addi, *et al.*, Phytochemical analysis, α-Glucosidase and α-Amylase inhibitory activities and acute toxicity studies of extracts from pomegranate (Punica granatum) bark, a valuable agro-industrial by-product, *Foods*, 2022, **11**(9), 1353.
50 C. Sarikurkcu, B. Kirkan, M. S. Ozer, O. Ceylan, N. Atilgan, M. Cengiz, *et al.*, Chemical characterization and biological activity of Onosma gigantea extracts, *Ind. Crops Prod.*, 2018, **115**, 323–329.
51 F. Payan, Structural basis for the inhibition of mammalian and insect α-amylases by plant protein inhibitors, *Biochim. Biophys. Acta, Proteins Proteomics*, 2004, **1696**(2), 171–180.
52 S. Sansenya and A. Payaka, Inhibitory potential of phenolic compounds of Thai colored rice (Oryza sativa L.) against α-

glucosidase and α-amylase through in vitro and in silico studies, *J. Sci. Food Agric.*, 2022, **102**(14), 6718–6726.

53 X. Li, Y. Bai, Z. Jin and B. Svensson, Food-derived non-phenolic α-amylase and α-glucosidase inhibitors for controlling starch digestion rate and guiding diabetes-friendly recipes, *Lwt*, 2022, **153**, 112455.

54 L. Zhang, Z.-c. Tu, T. Yuan, H. Wang, X. Xie and Z.-f. Fu, Antioxidants and α-glucosidase inhibitors from Ipomoea batatas leaves identified by bioassay-guided approach and structure-activity relationships, *Food Chem.*, 2016, **208**, 61–67.

55 S. G. Tumilaar, A. Hardianto, H. Dohi and D. Kurnia, A comprehensive review of free radicals, oxidative stress, and antioxidants: Overview, clinical applications, global perspectives, future directions, and mechanisms of antioxidant activity of flavonoid compounds, *J. Chem.*, 2024, **2024**(1), 5594386.

56 W. Widowati, N. Fauziah, H. Herdiman, M. Afni, E. Afifah, H. S. W. Kusuma, *et al.*, Antioxidant and anti aging assays of Oryza sativa extracts, vanillin and coumaric acid, *J. Nat. Rem.*, 2016, **16**(3), 88–99.

57 M. Platzer, S. Kiese, T. Tybussek, T. Herfellner, F. Schneider, U. Schweiggert-Weisz, *et al.*, Radical scavenging mechanisms of phenolic compounds: A quantitative structure-property relationship (QSPR) study, *Front. Nutr.*, 2022, **9**, 882458.

58 I. Bayram and E. A. Decker, Underlying mechanisms of synergistic antioxidant interactions during lipid oxidation, *Trends Food Sci. Technol.*, 2023, **133**, 219–230.

59 M. Kafali, M. A. Finos and A. Tsoupras, Vanillin and its derivatives: a critical review of their anti-inflammatory, anti-infective, wound-healing, neuroprotective, and anti-cancer health-promoting benefits, *Nutraceuticals*, 2024, **4**(4), 522–561.

60 A. Tai, T. Sawano, F. Yazama and H. Ito, Evaluation of antioxidant activity of vanillin by using multiple antioxidant assays, *Biochim. Biophys. Acta, Gen. Subj.*, 2011, **1810**(2), 170–177.

61 I. Kiliç and Y. Yeşiloğlu, Spectroscopic studies on the antioxidant activity of p-coumaric acid, *Spectrochim. Acta, Part A*, 2013, **115**, 719–724.